NeuroImage 223 (2020) 117302

Contents lists available at ScienceDirect

NeuroImage

journal homepage: www.elsevier.com/locate/neuroimage

Experience-dependent modulation of the visual evoked potential: Testing effect sizes, retention over time, and associations with age in 415 healthy individuals

Mathias Valstad[a,*], Torgeir Moberget[a,b], Daniël Roelfs[a], Nora B. Slapø[a], Clara M.F. Timpe[a,b], Dani Beck[a,b], Geneviève Richard[a], Linn Sofie Sæther[a], Beathe Haatveit[a], Knut Andre Skaug[a,c], Jan Egil Nordvik[d], Christoffer Hatlestad-Hall[b,e], Gaute T. Einevoll[f,g], Tuomo Mäki-Marttunen[a,h], Lars T. Westlye[a,b], Erik G. Jönsson[a,i], Ole A. Andreassen[a], Torbjørn Elvsåshagen[a,e,*]

[a] NORMENT, Division of Mental Health and Addiction, Oslo University Hospital & Institute of Clinical Medicine, University of Oslo, Norway
[b] Department of Psychology, University of Oslo, Oslo, Norway
[c] MentisCura, Reykjavik, Iceland
[d] CatoSenteret Rehabilitation Center, Son, Norway
[e] Department of Neurology, Oslo University Hospital, Oslo, Norway
[f] Faculty of Science and Technology, Norwegian University of Life Sciences, Ås, Norway
[g] Department of Physics, University of Oslo, Oslo, Norway
[h] Simula Research Laboratory, Oslo, Norway
[i] Department of Clinical Neuroscience, Centre for Psychiatric Research, Karolinska Institutet, Stockholm, Sweden

A B S T R A C T

Experience-dependent modulation of the visual evoked potential (VEP) is a promising proxy measure of synaptic plasticity in the cerebral cortex. However, existing studies are limited by small to moderate sample sizes as well as by considerable variability in how VEP modulation is quantified. In the present study, we used a large sample (n = 415) of healthy volunteers to compare different quantifications of VEP modulation with regards to effect sizes and retention of the modulation effect over time. We observed significant modulation for VEP components C1 (Cohen's d = 0.53), P1 (d = 0.66), N1 (d=-0.27), N1b (d=-0.66), but not P2 (d = 0.08), and in three clusters of total power modulation, 2–4 min after 2 Hz prolonged visual stimulation. For components N1 (d=-0.21) and N1b (d=-0.38), as well for the total power clusters, this effect was retained after 54–56 min, by which time also the P2 component had gained modulation (d = 0.54). Moderate to high correlations ($0.39 \leq \rho \leq 0.69$) between modulation at different postintervention blocks revealed a relatively high temporal stability in the modulation effect for each VEP component. However, different VEP components also showed markedly different temporal retention patterns. Finally, participant age correlated negatively with C1 (χ^2=30.4), and positively with P1 modulation (χ^2=13.4), whereas P2 modulation was larger for female participants (χ^2=15.4). There were no effects of either age or sex on N1 and N1b potentiation. These results provide strong support for VEP modulation, and especially N1b modulation, as a robust measure of synaptic plasticity, but underscore the need to differentiate between components, and to control for demographic confounders.

1. Introduction

Due to the essential role of synaptic plasticity in learning and memory (Takeuchi et al., 2013), as well as its likely role in the etiology of a range of psychiatric disorders (Schizophrenia Working Group of the Psychiatric Genomics Consortium, 2014; Stephan et al., 2006), several non-invasive methodologies for studying long term potentiation (LTP)-like synaptic plasticity in humans have been developed. Among these approaches, the application of high frequency or prolonged visual stimulation to manipulate visual evoked potentials (VEPs) measured using electroencephalography (EEG) has proven especially promising (Cooke and Bear, 2012). Supporting the utility of this experimental paradigm in clinical research, modulation of VEP components after high frequency or prolonged visual stimulation appears to be altered in mood (Elvsåshagen et al., 2012; Normann et al., 2007) and psychotic illnesses (Çavuş et al., 2012). However, the specific VEP components exhibiting robust modulation effects and differences between patients and controls, as well as the retention of modulation effects, have varied between studies, highlighting a need for further characterization of VEP modulation induced by prolonged visual stimulation in a large sample of healthy individuals.

In a standard VEP modulation paradigm, subjects are exposed first to VEP eliciting checkerboard (e.g. Normann et al., 2007) or grating stimuli (e.g. McNair et al., 2006), presented either as a phase reversal (e.g. Normann et al., 2007) or as a pattern onset with interstimulus intervals (e.g. Teyler et al., 2005). Then, subjects are exposed to a prolonged

* Corresponding authors at: Norwegian center for Mental Disorders Research, Oslo University Hospital, PoBox 4956 Nydalen, Norway.
E-mail addresses: mathias.valstad@medisin.uio.no (M. Valstad), torbjorn.elvsashagen@medisin.uio.no (T. Elvsåshagen).

https://doi.org/10.1016/j.neuroimage.2020.117302
Received 6 February 2020; Received in revised form 12 August 2020; Accepted 18 August 2020
Available online 20 August 2020

Table 1
Overview of VEP modulation studies.

Author, year[a]	N[b]	P.[c]	Intervention	Modulation[d]
Teyler et al., 2005	6	po	2 min 9 Hz checkerboard	N1b$^{\downarrow}$
McNair et al., 2006	10	po	2 min 8.6 Hz grating	N1b$^{\downarrow}$
Normann et al., 2007	32	pr	10 min 2 Hz checkerboard	C1$^{\uparrow}$, P1$^{\uparrow}$, N1$^{\downarrow}$
Ross et al., 2008	18	po	2 min 8.6 Hz grating	N1b$^{\downarrow}$
Çavuş et al., 2012	41	po	2 min 8.87 Hz checkerboard	C1$^{\downarrow}$, N1b$^{\downarrow}$
Elvsåshagen et al., 2012	66	pr	10 min 2 Hz checkerboard	P1$^{\uparrow}$, N1$^{\downarrow}$
Forsyth et al., 2015	65	po	2 min 8.87 Hz checkerboard	C1$^{\uparrow}$, P2$^{\uparrow}$
de Gobbi-Porto et al., 2015	17	po	2 min 9 Hz checkerboard	N1b$^{\downarrow}$
Klöppel et al., 2015	37	pr	10 min 2 Hz checkerboard	C1$^{\uparrow}$, P1$^{\uparrow}$
Smallwood et al., 2015	21	po	2 min 8.6 Hz grating	N1b$^{\downarrow}$
Forsyth et al., 2017	45	po	2 min 8.87 Hz checkerboard	C1$^{\uparrow}$, P2$^{\uparrow}$
Jahshan et al., 2017	64	po	2 min 8.87 Hz checkerboard	N1b$^{\downarrow}$, P2$^{\uparrow e}$
Wilson et al., 2017	24	po	2 min 9 Hz checkerboard	N1b$^{\downarrow}$
Spriggs et al., 2017	49	po	2 min 8.6 Hz grating	N1b$^{\downarrow}$, P2a$^{\uparrow}$
D'Souza et al., 2018	47	po	2 min 8.87 Hz checkerboard	[f]
Spriggs et al., 2018	40	po	2 min 9 Hz grating	C1$^{\downarrow}$, N1$^{\uparrow}$, P2$^{\uparrow}$
Sumner et al., 2018	20	po	2 min 9 Hz grating	P2$^{\uparrow}$
Zak et al., 2018	58	pr	10 min 2 Hz checkerboard	C1$^{\uparrow}$, P1$^{\uparrow}$, N1$^{\downarrow}$
Abuleil et al., 2019	47	po	2 min 9 Hz checkerboard	P1$^{\downarrow}$, N1b$^{\downarrow}$
Spriggs et al., 2019	28	po	2 min 8.6 Hz grating	N1b$^{\downarrow}$
Wynn et al., 2019	65	po	4 min of 10 Hz grating, on/off 5s	P1$^{\downarrow}$, N1b$^{\uparrow}$, P2$^{\uparrow e}$
Sumner et al., 2020	30	po	2 min 9 Hz grating	N1$^{\downarrow}$, P2$^{\uparrow}$

Table of studies using high frequency or prolonged visual stimulation to manipulate visual evoked potentials in humans.[a] Details in references. [b] Results for some participants may have been reported in more than one paper. [c] Presentation (P.) is either pattern onset (po), or phase reversal (pr). [d] Due to differing methods of analysis between studies, the exact nature of the modulated components can vary, and due to differences in statistical analysis between studies, the probability of actual modulation having been observed can also vary. Arrows denote direction of change pre-post intervention in the amplitude of a component (e.g. an upward arrow for a component that is negative at baseline means that the component became less negative or even positive after intervention). [e] The authors do not directly perform a component analysis. Component annotation is therefore tentative. [f] No significant modulation of the reported component.

(e.g. Normann et al., 2007) or high-frequency version (e.g. Teyler et al., 2005) of the checkerboard or grating stimulus. Lastly, after some delay, subjects are exposed to the initial stimulation again, which now typically evokes a significantly modulated visual potential. Importantly, the mechanisms underlying such experience-dependent VEP modulation seem to share many characteristics with LTP, thus having earned the placeholder epithet *LTP-like* plasticity. In mice, both *N*-methyl-D-aspartate receptor (NMDAR) antagonists like 3-(2-carboxypiperazin-4-yl)-propyl-1-phosphonic acid (CPP), and α-amino-3-hydroxy-5-methyl-4-isoxazolepropionic acid receptor (AMPAR) insertion-inhibitor GluR1-CT prevent experience-dependent VEP modulation from occurring (Frenkel et al., 2006). Also, electrical stimulation-induced LTP at thalamocortical synapses in the primary visual cortex (V1) enhances visual evoked potentials and inhibits further experience-dependent VEP modulation (Cooke and Bear, 2012). In humans, the spatial frequency- and orientation-specific receptive fields of V1 neurons have been exploited to demonstrate a specificity of experience-dependent VEP modulation that is consistent with the synaptic specificity characteristic of LTP (McNair et al., 2006; Ross et al., 2008).

Although most published studies have reported experience-dependent VEP modulation, the exact time windows and components modulated and the duration of modulation have varied between experiments (Table 1). In humans, the VEP is characterized by components separated in time, voltage polarity, and likely neural generators, with the largely negative C1 probably originating in the primary visual cortex (Di Russo, Martínez, Sereno, Pitzalis, and Hillyard, 2002) and occurring at ~50–90 ms post-stimulus, the positive P1 at ~80–120 ms and the negative N1 at ~130–200 ms, both probably originating in striate and extrastriate areas (Di Russo et al., 2002), and the positive and likely very complex P2 at ~200–300 ms post-stimulus. While some researchers (McNair et al., 2006; Ross et al., 2008; Teyler et al., 2005) demonstrated modulation of the relatively late-occurring N1b component exclusively, others have demonstrated an effect that is earlier and more widespread, with modulation of the P1 and N1 components (Elvsåshagen et al., 2012), and even of the C1 component (Çavuş et al., 2012; Normann et al., 2007). However, in these two studies demonstrating C1 modulation, opposite directions of effect were observed. The duration of VEP modulation has also varied between studies. Among the studies measuring VEP within the time range of classical LTP, that is, at least 30 min (Lisman, 2017) after prolonged or high frequency visual stimulation, one demonstrated retention of the modulation (Teyler et al., 2005), while another did not (Ross et al., 2008). Thus, it is also unclear to which extent early (< 30 min after high frequency or prolonged stimulation) and late (> 30 min after high frequency or prolonged stimulation) VEP modulation are associated, such that early VEP modulation could be taken as indicative of late VEP modulation. A substantial proportion of the observed differences between studies may be attributable to variations in experiment characteristics such as the specific visual stimulus used (grating or checkerboard), the presentation of the visual stimulus (pattern onset or phase reversal), the duration and frequency of stimulation at the intervention and at baseline assessments, as well as in the method of analysis employed. However, heterogeneity of results between studies that are similar in these respects seems to implicate error variance.

Indeed, some of the studies at hand may have been underpowered with respect to differentiation between modulation of separate VEP components, and may not have controlled for adequate confounders. Potential confounders of the VEP modulation effect include the age and sex of participants. With age, there is a general decline in neural plasticity in animals (Burke and Barnes, 2006). Using the VEP modulation paradigm in humans, visual cortical plasticity has been demonstrated in older individuals in one sample (de Gobbi-Porto et al., 2015), but not in another (Spriggs et al., 2017), and the relationship could be further elucidated with a continuous age distribution among participants. Fur-

ther, sex differences in anatomical features such as cortical gyrification (Luders et al., 2004) might impact orientation of neural tissue, electrical conduction, and ultimately scalp EEG signals. Another factor that could impact observed VEP modulation is the level of attention afforded the visual stimulus, especially during high frequency or prolonged visual stimulation, which might be indexed by visual stimulation-driven steady state responses (Çavuş et al., 2012). The impact of such potential confounders should be further characterized to adequately evaluate effects of high frequency or prolonged visual stimulation in different populations.

There are multiple possible ways of quantifying VEP modulation. For instance, while some researchers have focused on the N1b component of the VEP, which is typically operationalized as mean amplitude between the first negative and halfway to the first positive peak after P1 (e.g. McNair et al., 2006; Spriggs et al., 2017), others have focused on the N1 component, operationalized as the amplitude of the first negative peak after P1 (Elvsåshagen et al., 2012). Quantifications of VEP modulation to consider include changes from baseline amplitudes to postintervention amplitudes in the C1, P1, N1, N1b, and P2 components, as well as in the peak to peak difference P1-N1.

Since VEP modulation is likely to occur also outside of the electrodes and time windows to which classical VEP components are sensitive, some researchers have substituted or complemented component analyses with analyses across all channels and post-stimulus time points, while keeping false discovery rates low using permutation based inferential statistics (Jahshan et al., 2017; Wynn et al., 2019). Moreover, since some non-phase locked modulation, above and beyond the phase locked VEP modulation, might be present in the EEG after prolonged visual stimulation, time-frequency analyses of the post-stimulus EEG can be employed, complementing time-domain analyses, to further increase sensitivity.

Modulation of VEP components C1, P1, N1, N1b, and P2, as well as continuous modulations in the time and time-frequency domains have not been directly compared in a large sample of healthy individuals. It is therefore currently unknown which of the many potential indices of LTP-like synaptic plasticity is most sensitive and robust. Moreover, typical sample sizes within the field might make some studies vulnerable to winner's curse and random effects (Ioannidis, 2008). Here, we conducted the largest study of VEP modulation to date in 415 healthy volunteers and directly compared several quantifications of VEP modulation, enabling us to obtain realistic effect sizes and to determine which quantifications are best suited for indexing LTP-like synaptic plasticity in humans.

The present study had three main aims: first, to determine which EEG measures exhibit robust modulation following prolonged visual stimulation; second, to assess the retention of such VEP modulation effects over intervals reaching the time range of LTP, and the correlations between the magnitude of early and late VEP modulation; and third, to examine the extent to which age, sex, and markers of attention might influence VEP modulation.

2. Methods

2.1. Participants

415 participants were recruited to this study from Statistics Norway and announcements in national news outlets, and included after screening for psychiatric and somatic disorders in a semi-structured interview. We used the following exclusion criteria: a) a history of schizophrenia, bipolar disorder, or major depressive disorder, b) a history of chronic medical disorders, including cancer, cardiovascular disease, diabetes, and untreated hypertension, c) a history of neurological disorders, such as Parkinson's disease, epilepsy, and stroke, d) a history of moderate and severe head injuries with loss of consciousness >10 min, and e) first degree relative with SCZ, BD, or MDD. 59% of participants were female – their ages ranged from 18 to 83 years (mean = 49.7, sd = 16.2), while the ages of male participants ranged from 18 to 88 years (mean 47.9, sd = 17.8, see also Fig. 5). All participants had normal or corrected-to-normal vision. The experiment was approved by the Regional Ethical Committee of South-Eastern Norway, and all participants provided written informed consent.

2.2. Experimental procedures

The VEP modulation paradigm was adopted from Normann et al. (2007). Over a period of 67 min, 11 VEP blocks, i.e., 2 baseline blocks, 1 intervention block of prolonged visual stimulation, and 8 postintervention blocks, were presented on a 24 inch 144 Hz AOC LCD screen with 1 ms gray-to-gray response time (Fig. 1). All blocks, including the intervention block, consisted of a reversing checkerboard pattern with a spatial frequency of 1 cycle/degree over a ~28° visual angle. The reversal frequency was fixed at 2 reversals per second for the intervention block, whereas the baseline and postintervention blocks had jittered stimulus onset asynchronies of 500–1500 ms (mean = 1000 ms). All baseline and postintervention blocks lasted ~40 s (i.e., 40 checkerboard reversals), while the stimulation block lasted 10 min (i.e., 1200 reversals). Postintervention blocks were presented at 2 min, 3 min 40 s, 6 min 20 s, 8 min, ~30 min, ~32 min, ~54 min, and ~56 min after the intervention block. Through all blocks, the participants fixed their gaze on a red dot in the center of the screen, and pressed a key on a gaming controller when its color changed from red to green. Between the seventh and eight, and between the ninth and tenth blocks, participants underwent mismatch negativity (Näätänen et al., 1978) and prepulse inhibition (Graham and Murray, 1977) tasks, respectively.

2.3. Data acquisition

EEG recordings were acquired using a 64 channel BioSemi ActiveTwo amplifier, with Ag-AgCl sintered electrodes distributed across the scalp according to the international 10–20 system. External electrodes were placed at the outer canthi of both eyes (LO1, LO2), and below and above the left eye (IO1, SO1) in order to acquire horizontal and vertical electro-oculograms for eye movement and eye blink correction. Potentials at electrode sites were measured with respect to a common mode sense, with a driven right leg electrode minimizing common mode voltages, and sampled at 2048 Hz.

2.4. Signal processing

Signal processing was performed using MATLAB and the EEGLAB toolbox for MATLAB (Delorme and Makeig, 2004), while statistical analysis was performed using R version 3.6.0 (R Core Team, 2019). Offline, files were downsampled to 512 Hz. Noisy channels were identified with PrepPipeline algorithms (Bigdely-Shamlo et al., 2015) using default criteria, and removed. Remaining channels were first referenced to their common average voltage, before interpolation of removed channels from surrounding channel potentials, and finally all channels were rereferenced to the new common average after interpolation of bad channels. Data destined for time domain analysis were band-pass filtered between 0.1 and 40 Hz, while data for spectral analysis were high-pass filtered at 0.1 Hz. A fixed 20 ms delay in the visual presentation relative to the event markers was detected using a BioSemi PIN diode placed in front of the screen while running the paradigm, and event markers were adjusted offline to account for this. Next, epochs were extracted at 200 ms pre- to 500 ms post-stimulus. Muscle, eye blink and eye movement artifactual components were removed with SASICA defaults (Chaumon et al., 2015) after subjecting the epoched data to independent component analyses with the SOBI algorithm (Belouchrani et al., 1993). Then, epochs with amplitude diversions exceeding 100 μV were removed. Finally, all channels were referenced to the AFz electrode (however, one of the channel

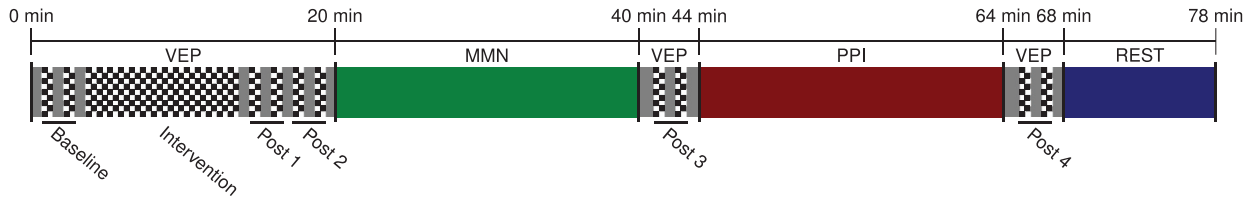

Fig. 1. Experimental timeline. **VEP**: visual evoked potential paradigm, **MMN**: mismatch negativity paradigm, **PPI**: prepulse inhibition paradigm, **REST**: resting state EEG.

by poststimulus latency analyses was performed directly on average referenced data).

2.5. Data analysis

Three different modes of EEG analysis were pursued: time domain analyses at group and individual levels, frequency domain analyses at the individual level, and time-frequency analyses at group and individual levels. Since the baseline consisted of two VEP blocks, postintervention blocks were also collapsed into series of two blocks for equal comparison, resulting in one baseline assessment and four postintervention assessments.

For time domain analysis, C1 was defined as minimum amplitude between 50 and 100 ms post-stimulus, P1 as maximum amplitude between 80 and 140 ms, N1 as the amplitude of the first negative peak after P1, N1b as mean amplitude between the first negative and halfway to the first positive peak after P1 (effectively 150–190 ms post-stimulus), and P2 as mean amplitude in the 50 ms after and including the first positive peak after P1 (effectively 228–278 ms post-stimulus), reflecting increased latency variabilities with later components. For a sensitivity analysis, and for all regression models, outliers in postintervention change from baseline were identified, within each component, according to the median absolute deviation procedure implemented in R package 'Routliers' (Delacre and Klein, 2019), yielding 28 outliers for C1, 19 for P1, 44 for N1, 19 for N1b, and 20 for P2, and removed within each component. Further, all channels were subjected to group-level component analysis, and the channel with highest amplitudes and most pronounced VEP component modulation (i.e., Oz) was selected for all later analyses (Fig. 3). In addition to these component analyses, we performed a completely data-driven, exploratory analysis, where voltages at each channel and each post-stimulus time point were calculated and assessed for postintervention changes, then subjected to permutation test-based (2000 simulations) strong control of the family wise error rate (Groppe et al., 2011).

For frequency domain analyses, entire continuous stretches of intervention block EEG were subjected to a Fast Fourier Transform (Cohen, 2014) before extraction of mean power within the narrow steady state band centered on the 2 Hz visual stimulation frequency (1.8–2.2 Hz).

For time-frequency analyses, high-pass filtered epochs from all participants were convolved with 5-cycle complex Morlet wavelets (Cohen, 2014) at each integer frequency between 10 and 120 Hz. Frequencies below 10 Hz were ignored due to the paradigm's relatively short stimulus onset asynchronies. Total power was then calculated as the median length of the resulting inner products within assessments, and inter-trial phase coherence was calculated as the length of the mean, within assessments, of $e^{i\theta}$ of the resulting inner product angles θ. Induced power was calculated as total power, except that each participant's ERP at each assessment was subtracted from each trial within that assessment before convolution. Total and induced power were then decibel converted with a baseline between 150 and 100 ms pre-stimulus. Finally, evoked power was calculated for each time and frequency within each assessment for each participant by subtracting decibel converted induced power from decibel converted total power. T-values for the change from baseline to the first postintervention assessment for all resulting pixels (representing a specific time-frequency combination) in total, evoked, and induced power, and inter-trial phase coherence, were then calculated, then subjected to permutation test-based (2000 simulations) strong control of the family wise error rate (Groppe et al., 2011). At the individual participant level, average values within the resulting clusters of modulation in total power, induced power, evoked power, and inter-trial phase coherence, were then extracted at all postintervention assessments.

2.6. Outcomes

Primary outcomes were i) modulation of components C1, P1, N1, N1b, and P2, and in the P1-N1 composite, between baseline and each postintervention assessment, as well as pairwise differences in modulation of components C1, P1, N1, N1b, and P2, ii) modulation, between baseline and postintervention assessments, in amplitudes at each channel and each post-stimulus latency between 0 and 500 ms, iii) modulation of within time-frequency clusters total power between baseline and each postintervention assessment, and a linear model for the effects of induced and evoked power for such differences, iv) correlations between baseline to postintervention amplitude changes for all components at all postintervention assessments, and v) effects of age, gender, and steady-state band powers during prolonged visual stimulation on the subsequent modulation of components C1, P1, N1, N1b, and P2.

Raw values are reported along with standard errors, calculated as standard deviations over the square root of the sample size. Baseline to postintervention changes (i.e., modulation effects), as well as differences in modulation between VEP components, are expressed as Cohen's d_z (henceforth denoted d), calculated as difference means over difference standard deviations (Cohen, 1988). In addition, modulation effects are expressed as response rates (rr), defined as the proportion of participants exhibiting the direction of baseline to postintervention changes that would be expected from average changes across participants. Pairwise comparisons between the modulation of different components was performed by permuting modulation scores, from throughout all postintervention assessments, across components, with switched polarity for components with negative mean modulation (i.e. N1 and N1b). Correlations are expressed as Spearman's ρ. Five regression models for C1, P1, N1, N1b, and P2 modulation scores were fitted using the general linear model, function glm() in R, with time (Post 1–4), age, gender, and intervention block steady state power as predictors. To avoid redundancy, since the effects of time are reported in other tests, we refrain from reporting regression model time effects. Further, one regression model for modulation of the first cluster of total power modulation was fitted, with corresponding clusters of evoked and induced power modulation as predictors. Model fit is indexed using Nagelkerke R^2, and effect is expressed as χ^2. P-values were calculated using the functions perm.test() or perm.cor.test() of R package 'jmuOutlier' (Garren, 2019), for differences and correlations, respectively, and the Anova function of R package 'car' (Fox and Weisberg, 2019) for regression models. Alpha levels were adjusted to control for multiple comparisons according to the effective number of independent comparisons, derived using eigenvalues of the correlation matrix of the entire continuous data set (Li and Ji, 2005), yielding an experiment-wide significance threshold at $\alpha = 7.2 \times 10^{-4}$.

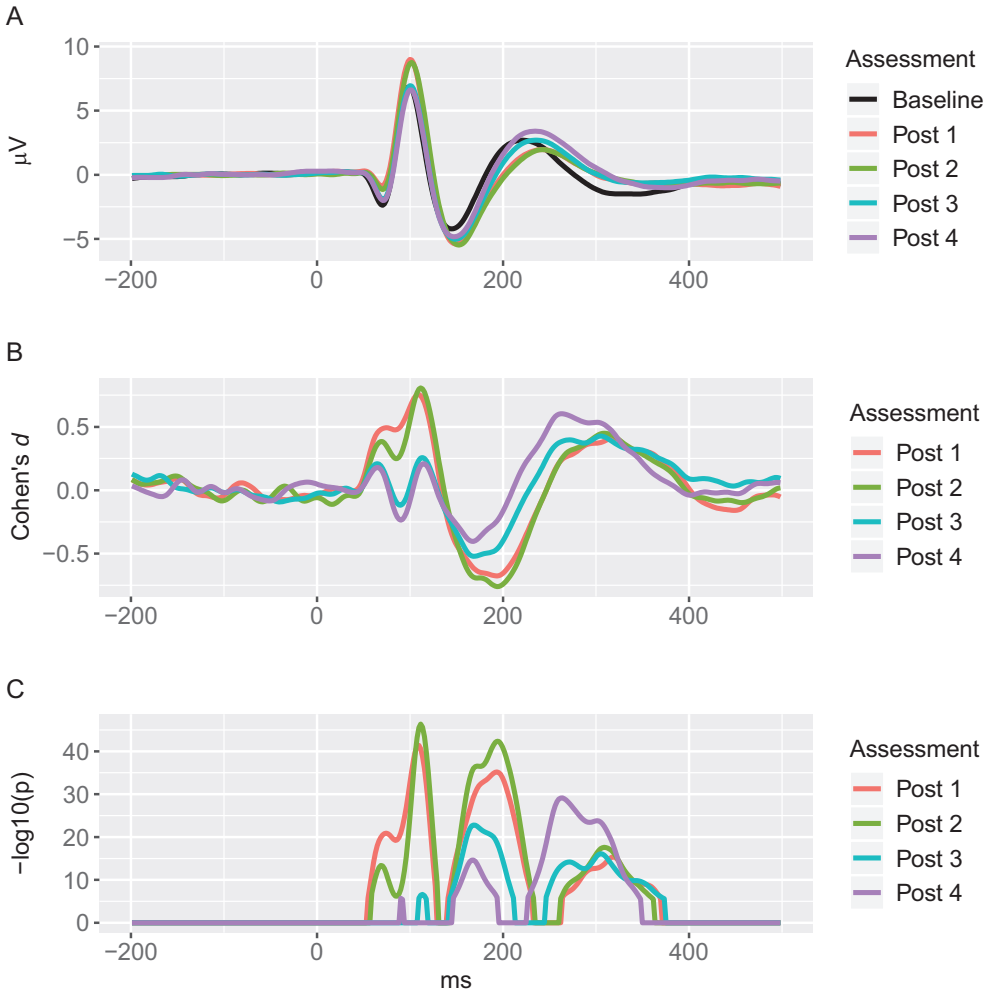

Fig. 2. **A.** Grand average visual evoked potentials measured at the occiput (Oz) with anterior reference (AFz) at baseline, post 1 (2–4 min after prolonged visual stimulation), post 2 (6–8 min), post 3 (30–32 min), and post 4 (54–56 min). **B.** Cohen's *d* from baseline VEP to the postintervention assessments. **C.** P-values for the difference between baseline VEP and each of the postintervention assessments, thresholded (i.e. significant if non-zero) according to permutation test-based (2000 simulations) strong control of the family wise error rate, and log transformed for visualization purposes.

Table 2
VEP component amplitudes and latencies at baseline.

Component	Latency (ms)	Amplitude (μV)
C1	66.6 ± 0.51	−3.91±0.24
P1	99.0 ± 0.41	8.42±0.30
N1	140.3 ± 0.81	−5.92±0.24
N1b	NA	−1.65±0.20
P2	NA	1.41±0.17

Table of VEP component amplitudes and latencies at baseline, measured at the occiput (Oz) with anterior reference (AFz). NA: not applicable.

3. Results

3.1. VEP modulation after prolonged visual stimulation

The checkerboard reversal stimulation evoked the expected C1, P1, N1, and P2 components of the VEP (Fig. 2; see Table 2 for latencies and amplitudes). Initial group level analyses demonstrated that, across VEP components, the highest amplitudes and the largest modulation effects were exhibited at the occipital Oz electrode (Fig. 3A-B), which was accordingly selected for individual level analyses.

When testing for modulation effects across all timepoints of the VEP at the first postintervention assessment after prolonged visual stimulation, significant changes at latencies of 55–127 ms, 141–231 ms, and 264–369 ms were observed at the occiput (Oz) (Fig. 2), with related changes at other channels at comparable time windows (Fig. 4). Correspondingly, experience-dependent VEP modulation was apparent as amplitude changes from baseline to the first postintervention assessment for both the C1 (d = 0.53, rr = 0.70), P1 (d = 0.66, rr = 0.76), N1 (d = −0.27, rr = 0.62), N1b (d = −0.66, rr = 0.77), but not P2 (d = 0.08, p = 0.10, rr = 0.53) components, with highly similar effects for both the C1 (d = 0.44, rr = 0.67), P1 (d = 0.55, rr = 0.72), N1 (d = −0.26, rr = 0.61), N1b (d = −0.71, rr = 0.77) and the P2 (d = 0.08, p = 0.10, rr = 0.54) components at the immediately following second postintervention assessment. Some, but not all, changes after prolonged visual stimulation were retained at the third and fourth postintervention assessments. C1 modulation was significant at the third postintervention assessment (d = 0.20, rr = 0.58), but failed to pass corrected alpha thresholds at the fourth postintervention assessment (d = 0.16, p = 0.001, rr = 0.56). The P1 component did not retain modulation at the third (d = 0.04, p = 0.36, rr = 0.54), nor at the fourth (d = −0.06, p = 0.22, rr = 0.48) postintervention assessment. The N1 component retained modulation at the third (d = −0.17, rr = 0.60), and fourth (d = −0.21, rr = 0.66) postintervention assessment. The N1b component retained modulation at both the third (d = −0.53, rr = 0.75), and the fourth (d = −0.38, rr = 0.68) postintervention assessment. Finally, the P2 component gained modulation at the third (d = 0.30, rr = 0.65) and the fourth (d = 0.54, rr = 0.75) postintervention assessment (Table 3, Fig. 3). Almost all of these results, the only exception being retention of C1 modulation at the third postintervention assessment, were reproduced with outliers removed (Table S1).

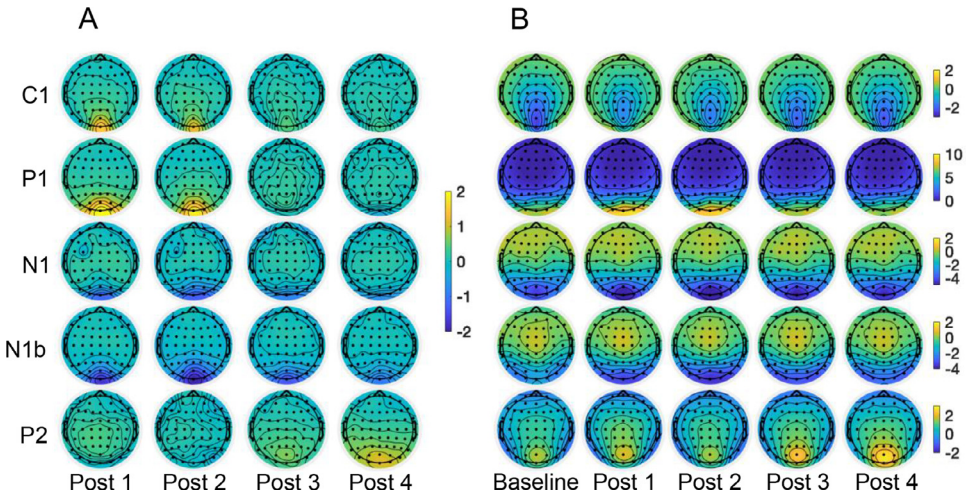

Fig. 3. A. Scalp topographical distribution of C1, P1, N1, N1b, and P2 unscaled amplitude differences (in μV) from baseline to postintervention assessments 1 (2–4 min after prolonged visual stimulation), 2 (6–8 min), 3 (30–32 min), and 4 (54–56 min). **B.** Scalp topographical distribution of C1, P1, N1, N1b, and P2 amplitudes at baseline and each of the postintervention assessments 1–4.

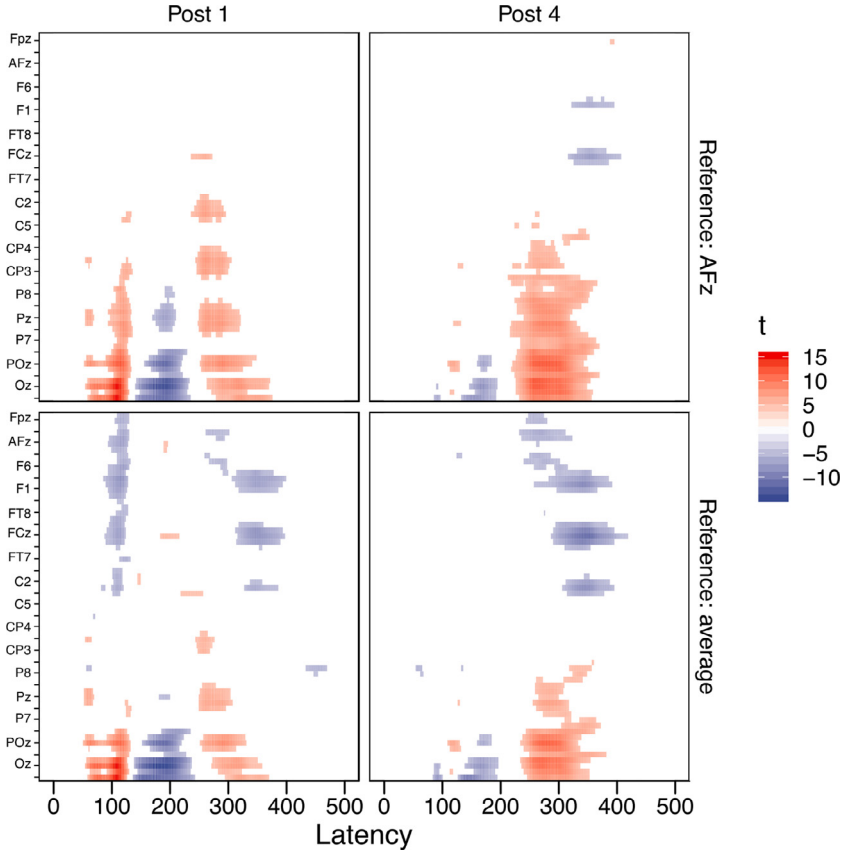

Fig. 4. Four panels displaying VEP modulation (expressed as t-scores, thresholded according to permutation test-based strong control of the family wise error rate) across poststimulus latencies (x-axis) and channels (y-axis). The first column of panels display modulation at postintervention assessment post 1 (2–4 min after prolonged visual stimulation). The second column of panels display modulation at postintervention assessment post 4 (54–56 min). The first row of panels display modulation with an AFz reference. The second row of panels display modulation with an average reference. Channels are ordered from nasion to inion.

Data-driven time-domain analyses revealed a cluster of positive modulation to which components C1 and P1 would be sensitive, and a cluster of negative modulation to which components N1 and N1b would be sensitive. Further, a large cluster of positive modulation was centered at a latency around ~300 ms poststimulus, to which the P2 component would only be partially sensitive (Fig. 4).

Permutation of modulation scores in a pairwise manner, across components C1, P1, N1, N1b, and P2, demonstrated significant differences in modulation in 5 out of 10 comparisons. First, P1 modulation was larger than P2 modulation ($d = 0.09$, $p = 0.0001$). Further, N1b modulation was larger than modulation of all other components, including C1 ($d = 0.18$, $p < 5 \times 10^{-5}$), P1 ($d = 0.12$, $p < 5 \times 10^{-5}$), N1 ($d = 0.34$, $p < 5 \times 10^{-5}$), and P2 ($d = 0.20$, $p < 5 \times 10^{-5}$).

The P1-N1 composite exhibited significant modulation at the first ($d = 0.70$, rr = 0.80), second ($d = 0.60$, rr = 0.78), and third ($d = 0.19$, rr = 0.61), but not the last ($d = 0.14$, rr = 0.60) postintervention assessment.

3.2. Within assessments changes in the VEP

There were also differences between component amplitudes within assessments (Fig. 6), with significant changes from the first to the second baseline block (i.e. within the baseline assessment) for components P1 ($d = 0.21$), N1 ($d = -0.32$), N1b ($d = -0.28$), and P2 ($d = 0.17$), from the first to the second postintervention block (i.e. within the first postintervention assessment) for components C1 ($d = 0.18$), N1 ($d = 0.24$), and from the seventh to the eighth postintervention block (i.e. within the fourth postintervention assessment) for components C1 ($d = 0.24$), P1 ($d = 0.31$), N1 ($d = -0.19$), and N1b ($d = -0.35$). These effects were weaker than effects of the prolonged visual stimulation for components

Table 3
VEP component modulation after prolonged visual stimulation.

		C1	P1	N1	N1b	P2
Post 1 (2–4 min)	*d*	0.53	0.66	−0.27	−0.66	0.08
	rr	0.70	0.76	0.62	0.77	0.53
	p	$<5 \times 10^{-5}$	$<5 \times 10^{-5}$	$<5 \times 10^{-5}$	$<5 \times 10^{-5}$	0.10
	-log(p*)	23.1	33.7	7.1	33.7	1
Post 2 (6–8 min)	*d*	0.44	0.55	−0.26	−0.71	0.08
	rr	0.67	0.72	0.61	0.77	0.54
	p	$<5 \times 10^{-5}$	$<5 \times 10^{-5}$	$<5 \times 10^{-5}$	$<5 \times 10^{-5}$	0.10
	-log(p*)	16.9	24.6	6.8	37.8	1
Post 3 (30–32 min)	*d*	0.20	0.04	−0.17	−0.53	0.30
	rr	0.58	0.54	0.60	0.75	0.65
	p	$<5 \times 10^{-5}$	0.38	0.0003	$<5 \times 10^{-5}$	$<5 \times 10^{-5}$
	-log(p*)	4.16	0.4	3.2	23.0	8.9
Post 4 (54–56 min)	*d*	0.16	−0.06	−0.21	−0.38	0.54
	rr	0.56	0.48	0.66	0.68	0.75
	p	0.001	0.22	$<5 \times 10^{-5}$	$<5 \times 10^{-5}$	$<5 \times 10^{-5}$
	-log(p*)	2.9	0.7	4.8	12.9	24.3

Table of VEP component modulation after prolonged visual stimulation. **d**: Cohen's d, **rr**: response rate, **p**: p-value after 20,000 permutations, **-log(p*)**: negative decimal logarithm of *t*-test p-value (for illustration, not all modulations are normally distributed).

Table 4
Time-frequency cluster modulation after prolonged visual stimulation.

		A1	A2	A3	I1	E1	ITPC1	ITPC2
Post 1 (2–4 min)	*d*	−0.51	−0.26	−0.27	−0.27	−0.23	−0.41	−0.33
	rr	0.73	0.66	0.61	0.62	0.59	0.64	0.62
	p	$<5 \times 10^{-5}$	$<5 \times 10^{-5}$	$<5 \times 10^{-5}$	$<5 \times 10^{-5}$	$<5 \times 10^{-5}$	$<5 \times 10^{-5}$	$<5 \times 10^{-5}$
	-log(p*)	20.9	6.6	7.0	7.0	5.2	14.2	9.6
Post 2 (6–8 min)	*d*	−0.55	−0.21	−0.18	−0.32	−0.29	−0.39	−0.26
	rr	0.74	0.58	0.58	0.62	0.64	0.68	0.64
	p	$<5 \times 10^{-5}$	$<5 \times 10^{-5}$	0.0003	$<5 \times 10^{-5}$	$<5 \times 10^{-5}$	$<5 \times 10^{-5}$	$<5 \times 10^{-5}$
	-log(p*)	23.8	4.6	3.4	9.3	7.9	12.9	6.6
Post 3 (30–32 min)	*d*	−0.48	−0.32	−0.29	−0.23	−0.20	−0.31	−0.24
	rr	0.72	0.61	0.63	0.60	0.57	0.63	0.62
	p	$<5 \times 10^{-5}$	$<5 \times 10^{-5}$	$<5 \times 10^{-5}$	$<5 \times 10^{-5}$	0.0001	$<5 \times 10^{-5}$	$<5 \times 10^{-5}$
	-log(p*)	19.1	9.4	7.74	5.0	4.0	8.7	5.5
Post 4 (54–56 min)	*d*	−0.38	−0.24	−0.29	−0.08	−0.27	−0.32	−0.10
	rr	0.66	0.61	0.64	0.54	0.62	0.62	0.56
	p	$<5 \times 10^{-5}$	$<5 \times 10^{-5}$	$<5 \times 10^{-5}$	0.12	$<5 \times 10^{-5}$	$<5 \times 10^{-5}$	0.046
	-log(p*)	12.4	5.7	7.9	0.9	6.8	9.1	1.3

Table of cluster power modulations after prolonged visual stimulation. **d**: Cohen's *d*, **rr**: response rate, **p**: p-value after 20,000 permutations, **-log(p*)**: negative decimal logarithm of *t*-test p-value (for illustration, not all potentiations are normally distributed), **A1–3**: Total power modulation clusters, **I1**: Induced power modulation cluster, **E2**: Evoked power cluster. **ITPC1–2**: Intertrial phase coherence clusters.

C1 ($p = 2.1 \times 10^{-5}$), N1b ($p = 3.0 \times 10^{-14}$), and P2 ($p = 2.6 \times 10^{-6}$), but not for components P1 ($p = 0.10$) or N1 ($p = 0.004$; two-tailed tests).

3.3. Clusters of time-frequency power modulation after prolonged visual stimulation

The time-frequency analysis exploring the main effect of prolonged visual stimulation yielded three clusters of significant modulation of total power, the first centered around ~26 Hz and 65 ms post-stimulus, the second centered around ~15 Hz and 245 ms post-stimulus, and the third centered around ~12 Hz and 229 ms post-stimulus (Fig. 7). Results from analyses using individual participants' values averaged within clusters of modulation of total power, as well as induced power, evoked power, and inter-trial phase coherence, are presented in Table 4. These analyses revealed that modulation of the first total power cluster was significant at all postintervention assessments, including the first ($d = -0.51$, rr = 0.73), second ($d = -0.55$, rr = 0.74), third ($d = -0.48$, rr = 0.72), and fourth ($d = -0.37$, rr = 0.66). Further, modulation of the second total power component was also signficant at the first ($d = -0.26$, rr = 0.62), second ($d = -0.21$, rr = 0.58), third ($d = -0.32$, rr = 0.61), and fourth ($d = -0.24$. rr = 0.61) postintervention assessments. Finally, modulation of the third total power component was significant at the first, second, and fourth, but not the third, postintervention assessment. The first total power cluster overlapped with an induced power cluster and a separate evoked power cluster, and the power reduction within this cluster after prolonged visual stimulation was reasonably well modelled ($R^2 = 0.38$) by power changes in the corresponding evoked ($\chi^2 = 26.4$, $p = 2.8 \times 10^{-7}$) and especially induced ($\chi^2 = 154.3$, $p = 2.0 \times 10^{-35}$) cluster.

3.4. Associations between VEP modulation across components and assessments

Correlations across assessments for baseline to postintervention modulation effects were moderate within components C1 ($0.47 \leq \rho \leq 0.69$), P1 ($0.39 \leq \rho \leq 0.67$), N1 ($0.42 \leq \rho \leq 0.62$), N1b ($0.44 \leq \rho \leq 0.66$), and P2 ($0.45 \leq \rho \leq 0.60$) (Fig. 8). All correlations above and including $r = 0.17$ remained significant after multiple comparison correction.

3.5. Associations between VEP modulation and age, sex, and intervention block steady state power

The regression model for C1 modulation revealed effects of age ($\chi^2 = 30.4$, $p = 3.5 \times 10^{-8}$), with modulation decreasing with higher

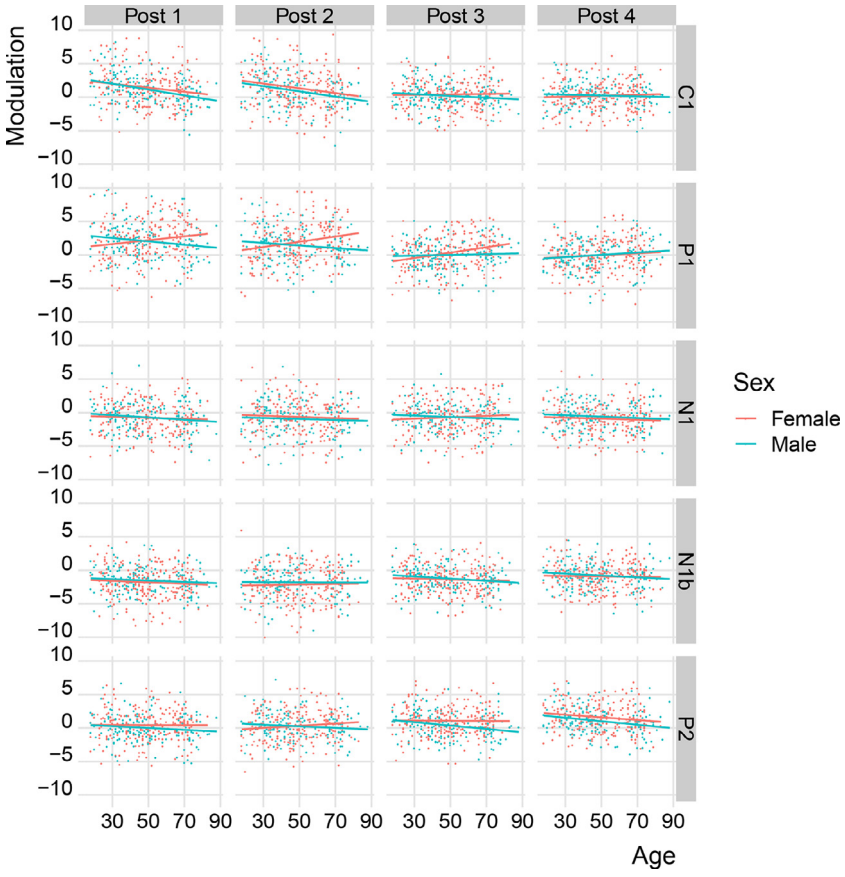

Fig. 5. Distributions of amplitude differences (in μV) between baseline and postintervention assessments post 1 (2–4 min after prolonged visual stimulation), post 2 (6–8 min), post 3 (30–32 min), and post 4 (54–56 min), and their associations with age (in years) by sex, for VEP components C1, P1, N1, N1b, and P2. Linear regression showed significant associations between age and C1 modulation ($\chi^2 = 30.4$, $p = 3.5 \times 10^{-8}$), age and P1 modulation ($\chi^2 = 13.4$, $p = 2.6 \times 10^{-4}$), and sex and P2 modulation ($\chi^2 = 15.4$, $p = 8.5 \times 10^{-5}$). Outliers not included.

age (Fig. 5), but not of sex ($p = 0.07$) or intervention steady state power ($p = 0.76$). The regression model for P1 modulation revealed effects of age ($\chi^2 = 13.4$, $p = 2.6 \times 10^{-4}$), with modulation increasing with higher age, but not of sex ($p = 0.10$) or intervention steady state power ($p = 0.76$). The regression model for N1 modulation revealed no significant effects of either age ($p = 0.05$), sex ($p = 0.88$) or intervention steady state power ($p = 0.03$). Similarily, the regression model for N1b modulation revealed no significant effects of either age ($p = 0.03$), sex ($p = 0.05$), or intervention steady state power ($p = 0.21$). Finally, the regression model for P2 modulation revealed no significant effects of age ($p = 0.002$), but significant effects of sex ($\chi^2 = 15.4$, $p = 8.5 \times 10^{-5}$), and intervention steady state power ($\chi^2 = 11.7$, $p = 6.2 \times 10^{-4}$), with greater modulation for female participants and participants with higher intervention steady state power, respectively. For the attentional task, we only obtained hit rate data for 45.8% of participants, due to error in the gaming controller. Thus, we performed a set of control analyses to ensure that the participants for which attentional data was not obtained did not differ from the participants for which attentional data was obtained. These showed that there was no difference between these groups in P1, N1, N1b, or P2 modulation, but only a nominal difference in C1 modulation ($p = 0.04$), and that clear VEPs were evoked for 96% of participants for which attentional data was not obtained. Among participants for which attentional data was obtained, the mean hit rate was 98.4%. Together, these results indicate overall satisfying levels of attention.

4. Discussion

The current study yielded four main findings. First, we demonstrate robust experience-dependent modulation of the visual evoked potential in a large sample of healthy volunteers ($n = 415$). Second, the retention of this modulation effect over time varied across VEP components, strongly suggesting that VEP modulation is not a unitary phenomenon and likely involves several different plasticity mechanisms. Third, age and sex, as well as intervention steady state power, emerged as significantly associated with some, but not all, quantifications of VEP modulation. Finally, we identify the N1b component as the most sensitive quantification of VEP modulation.

4.1. Experience-dependent modulation of visual evoked potentials

At the first and second postintervention assessments, respectively 2 and 6 min after prolonged visual stimulation, moderate to strong modulation was observed in VEP components C1, P1, N1, and N1b, as well as in the composite P1-N1. Such experience-dependent modulations have previously been shown to share many characteristics with LTP, including NMDAR-dependence (Frenkel et al., 2006), post-synaptic AMPAR insertion dependence (Frenkel et al., 2006), and stimulus specificity (McNair et al., 2006; Ross et al., 2008), and have therefore been regarded as indices of LTP-like cortical synaptic plasticity.

In the present study, some widely used quantifications of VEP modulation – modulations of the C1, P1, N1, and N1b components – coincide in latency with clusters of modulation as revealed by data-driven time domain analyses. On the other hand, we have shown that a large time-domain cluster of modulation, centered around a post-stimulus latency of ~300 ms and expanding in time in later postintervention assessments, is not very well captured by the P2 component. An important caveat, however, is that such results might not be immediately generalizable to different VEP modulation paradigms, such as those using pattern onset sine gratings rather than checkerboard reversals.

Time-frequency analyses also revealed modulation of total power in three time-frequency clusters, all of which exhibited effects of prolonged visual stimulation that were comparable to effects seen on time domain VEP components, and that, like N1 and N1b modulation, were retained

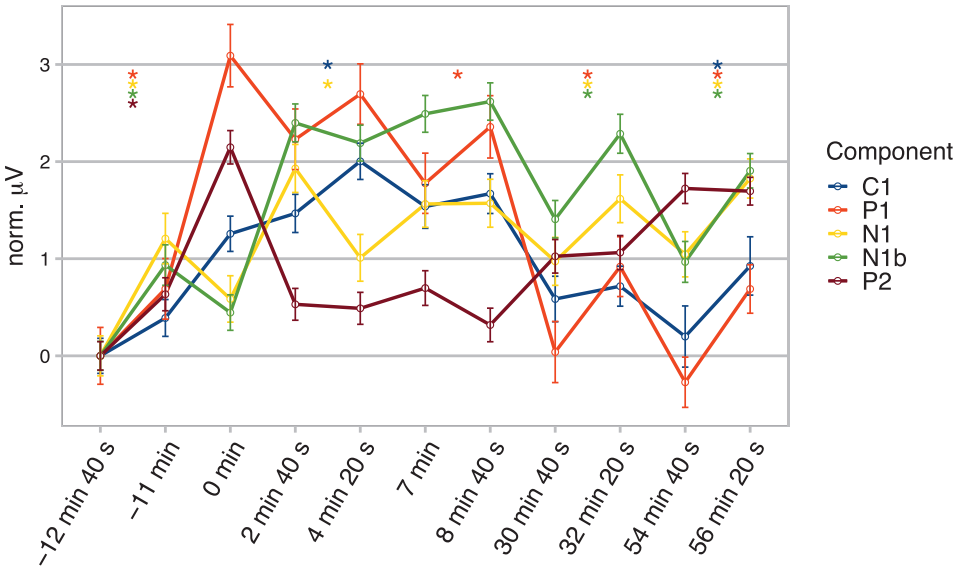

Fig. 6. Component amplitudes at separate checkerboard stimulation blocks, normalized to the first block, with error bars showing standard error of measurement. The polarity of N1 and N1b modulation has been flipped for easy comparison with modulation of the other components. Asterisks denote significant ($p < 7.2 \times 10^{-4}$) amplitude change within assessments, that is, within the baseline assessment (from the block at −12 min 40 s to the block at −11 min), within the first postintervention assessment (from the block at 2 min 40 s to the block at post at 4 min 20 s, and so on.

at ~54–56 min postintervention. The first cluster of time-frequency modulation, centered at ~65 ms and 26 Hz, overlapped with both clusters of evoked and clusters of induced modulation. Since modulation in induced power made the strongest contribution to modulation in total power, it is likely that the observed total power modulation might reflect neural dynamics to which time domain VEP modulations are not sensitive.

4.2. Experience-dependent VEP modulation: retention slopes and correlations

We observed differential response patterns between quantifications of VEP modulation, indicating differences in underlying mechanisms. Retention at the third and fourth postintervention assessments, i.e., ~30–32 and ~54–56 min after prolonged visual stimulation, was observed for components N1 and N1b. In contrast to N1 and N1b modulation, C1 modulation was not significantly retained at ~54–56 min postintervention. The retention of N1 and N1b modulation at 30 and 54 min postintervention is consistent with LTP-like synaptic processes as underlying mechanisms, since this duration goes beyond the usual decay of presynaptic short-term potentiation (Citri and Malenka, 2008; Regehr, 2012). Spearman correlations around 0.42–0.49 between N1 and N1b modulations at 2 and ~54–56 min postintervention suggest a connection between early and later modulation effects, which has been established for most forms of synaptic plasticity (Citri and Malenka, 2008), further corroborating the claim that N1 and N1b modulations reflect LTP-like cortical plasticity.

With a sharp voltage increase in the intervention block and subsequent return to near baseline in the first two postintervention assessments, and renewed amplitude increases in the third and last postintervention assessments (Figs. 5,6), the response pattern for the P2 component, similar to what has been observed previously (Forsyth et al., 2015; Forsyth et al., 2017), constitutes a clear exception. There is, already in the first two postintervention assessments, detectable modulation in the time-domain cluster adjacent to and partially overlapping with P2, but since this cluster is also expanding in time and in effect sizes from early to late postintervention assessments, the picture of growing effect is not contradicted. Although NMDAR-dependent LTP typically exhibits a gradual decay (Citri and Malenka, 2008), the response pattern for the P2 component is, however, not inconsistent with NMDAR-dependent LTP as a mechanism, since P2 modulation might summate across synaptic potentiation and depression with differential time ranges (Forsyth et al., 2015). Indeed, NMDAR agonist D-cycloserine has previously been shown to increase P2 modulation (Forsyth et al., 2015). Further, the P2 component appears to lack input specificity for some VEP modulation paradigms (Sumner et al., 2018), although this does not necessarily preclude input specificity for other, similar paradigms. Thus, we can not based on the present data exclude the possibility that the effect of time on P2 amplitudes might involve NMDAR-dependent LTP as a mechanism. Along similar lines, the retention slope of P1, with a complete decay between 6 and 30 min after prolonged visual stimulation, is also consistent with synaptic plasticity as underlying mechanism. For example, P1 modulation might reflect some short-term plasticity such as post-tetanic potentiation (Citri and Malenka, 2008). Further, the early P1 modulation might reflect an early phase of LTP, that at later stages present in a qualitatively different manner (Bosch et al., 2014), both at molecular and electrophysiological levels. For example, P2 modulation could potentially be related to later phases of the complex gene expression patterns and synaptic changes underlying LTP (Bosch et al., 2104), However, while these speculations might provide testable hypotheses for future research, it should be noted that they cannot be directly addressed in the present data. Indeed, the current results could be compatible with many different patterns of interaction between different forms of plasticity with opposing effects on the EEG.

4.3. Age, sex, and steady state power are associated with some, but not all, VEP components

Linear regression showed a negative main effect of age on C1 modulation, and a positive main effect of age on P1 modulation, suggesting that C1 modulation across postintervention assessments is reduced with age, while P1 modulation is increased with age. No effects of age were observed on modulation of either the N1, N1b, or the P2 components. These results are in line with a previous demonstration of robust VEP modulation among older individuals (de Gobbi-Porto et al., 2015). On the other hand, they seem to contrast with the lack of N1b modulation previously observed in older participants (Spriggs et al., 2017), and with the more general decline in neural plasticity associated with aging (Burke and Barnes, 2006). Further, regression models demonstrated larger increase in P2 amplitudes among female participants than among male participants. Together, these results underscore the need to differentiate between VEP components, and to control for demographic variables like age and sex, especially in case-control studies of VEP modulation.

Linear regression models also revealed an effect of intervention steady state power on P2 modulation, with higher P2 modulation among

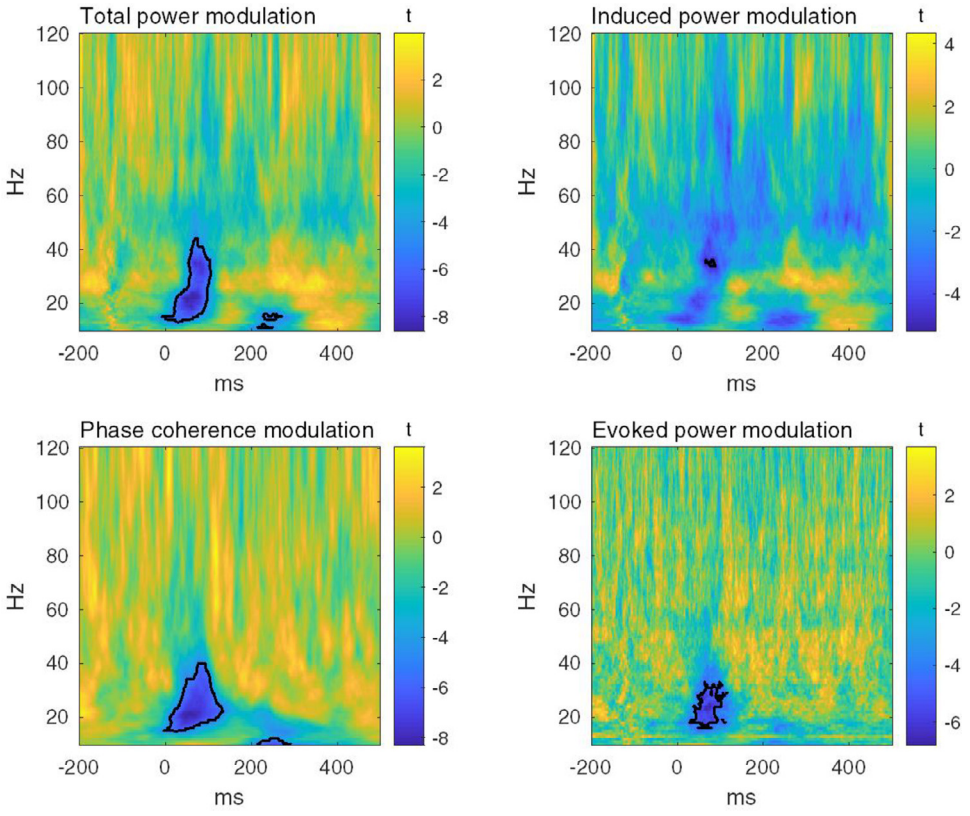

Fig. 7. Changes at the occiput (Oz) in total power, induced power, phase coherence, and evoked power, in frequencies 10–120 Hz, before to after prolonged visual stimulation, given as t-scores for each pixel. Significant clusters circumscribed with black lines.

participants with higher steady state power, but not on modulation of any of the other components. In a previous study of VEP modulation using 8.7 Hz visual stimulation (Çavuş et al., 2012), intervention block steady state power was associated with N1b modulation in healthy controls. Together, these results indicate that the degree of neural entrainment to prolonged or high frequency visual stimulation might impact the magnitude of VEP modulation.

4.4. Robust and enduring modulation of component N1b

Our quantifications of VEP modulation seem to be relatively specific in that they exhibit distinct effects, retention slopes and associations with age and sex. Modulation of the N1b component after prolonged visual stimulation was overall the strongest effect. Effect size differences, relatively high correlations, and comparable associations with age and sex between components N1 and N1b suggest that N1b quantifications of VEP modulation might be preferable, at least under conditions similar to those present in this study. Although some observed effects of time might have been caused by other experimental characteristics than the prolonged visual stimulation, the N1b component has repeatedly been shown to increase in amplitude with high frequency visual stimulation, and not without (Teyler et al., 2005), and not with visual stimulation of a different orientation (Ross et al., 2008) or spatial frequency (McNair et al., 2006), supporting the notion that at least N1b modulation is due to the high frequency or prolonged visual stimulation.

4.5. Possible influence of postintervention blocks on retention

In the present study we observed modulation of components C1, P1, N1, N1b, and P2 even between blocks of short duration checkerboard stimulation. Thus, there is reason to question whether the retention, especially for components N1 and N1b which exhibit long duration modulation, could have been increased by the postintervention stimulus blocks. Postintervention blocks have been shown to decrease retention of N1b modulation (Teyler et al., 2005), but with frequency differences between intervention and postintervention blocks (i.e. 9 vs 1 Hz) that were greater than in the present study (same mean frequency), so some influence in favor of retention cannot be ruled out with the present data.

4.6. Limitations

A limitation of this study is that frequencies below 10 Hz were not considered in the time-frequency analyses, due to the paradigm's relatively short stimulus onset asynchronies. Further, as we have only studied VEP modulation in one of several potential VEP modulation paradigms, generalization to other, similar paradigms, should be done with caution.

4.7. Conclusion

The results of the current study show robust modulation after prolonged visual stimulation in VEP components C1, P1, N1, and N1b, as well as in three time-frequency clusters of total power modulation. Moreover, we observed differential retention slopes, effect sizes, and associations to age and sex for the modulation of VEP components, strongly suggesting that VEP modulation is not a unitary phenomenon. Taken together with results from a series of invasive studies in rodents, our current results support the use of prolonged visual stimulation induced VEP modulation, and especially N1b modulation, as a robust, non-invasive index of LTP-like cortical plasticity in humans.

Credit author statement

Mathias Valstad: conceptualization, software, formal analysis, investigation, visualization, and writing – original draft.

Torgeir Moberget: conceptualization, methodology, writing – review & editing, and supervision

Daniël Roelfs: investigation and visualization

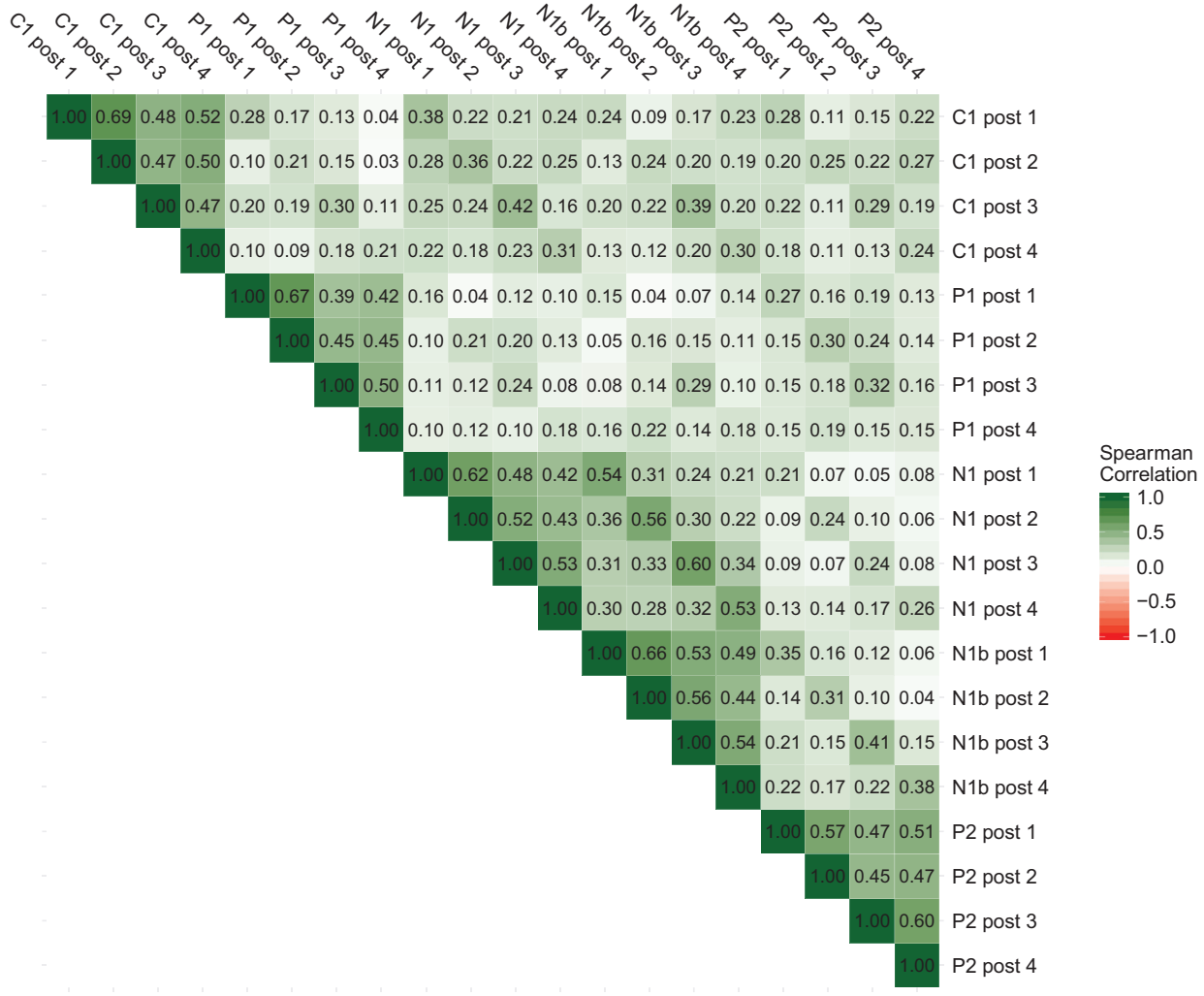

Fig. 8. Spearman's ρ correlations between modulations of VEP components C1, P1, N1, N1b, and P2 at postintervention assessments 1–4. Since these are correlations between raw modulation effects, some could, in principle, have been negative, but no negative correlations were found.

Nora B. Slapø: investigation
Clara M.F. Timpe: investigation
Dani Beck: investigation
Geneviève Richard: investigation
Linn Sofie Sæther: investigation
Beathe Haatveit: investigation
Knut Andre Skaug: investigation
Jan Egil Nordvik: project administration
Christoffer Hatlestad-Hall: software
Gaute T. Einevoll: conceptualization
Tuomo Mäki-Marttunen: conceptualization
Lars T. Westlye: project administration
Erik G. Jönsson: project administration
Ole A. Andreassen: conceptualization, project administration, writing – review & editing, and supervision
Torbjørn Elvsåshagen: conceptualization, methodology, investigation, writing – review & editing, supervision, project administration, and funding acquisition

Acknowledgments

This study was funded by the Research Council of Norway, the South-Eastern Norway Regional Health Authority, Oslo University Hospital (2015–078), and a research grant from Mrs. Throne-Holst. The authors report no biomedical financial interests or potential conflicts of interest.

Supplementary materials

Supplementary material associated with this article can be found, in the online version, at doi:10.1016/j.neuroimage.2020.117302.

References

Abuleil, D., McCulloch, D.L., Thompson, B., 2019. Older adults exhibit greater visual cortex inhibition and reduced visual cortex plasticity compared to younger adults. Front. Neurosci. 13, 607.
Belouchrani, A., Abed-Meraim, K., Cardoso, J.F., Moulines, E., 1993. Second order blind separation of temporally correlated sources. Proc. Int. Conf. Digital Signal Proc. 346–351.
Bigdely-Shamlo, N., Mullen, T., Kothe, C., Su, K.-M., Robbins, K.A., 2015. The PREP pipeline: standardized preprocessing for large-scale EEG analysis. Front. Neuroinform. 9, 16. http://doi.org/10.3389/fninf.2015.00016.
Bosch, M., Castro, J., Saneyoshi, T., Matsuno, H., Sur, M., Hayashi, Y, 2014. Structural and molecular remodeling of dendritic spine substructures during long-term potentiation. Neuron 82 (2), 444–459.
Burke, S.N., Barnes, C.A., 2006. Neural plasticity in the ageing brain. Nat. Rev. Neurosci. 7 (1), 30–40. http://doi.org/10.1038/nrn1809.
Chaumon, M., Bishop, D.V.M., Busch, N.A., 2015. A practical guide to the selection of independent components of the electroencephalogram for artifact correction. J. Neurosci. Methods 250, 47–63. http://doi.org/10.1016/j.jneumeth.2015.02.025.
Citri, A., Malenka, R.C., 2008. Synaptic plasticity: multiple forms, functions, and mechanisms. Neuropsychopharmacology 33 (1), 18–41. http://doi.org/10.1038/sj.npp.1301559.
Cohen, J., 1988. Statistical Power Analysis For the Behavioral Sciences, 2nd Lawrence Erlbaum Associates.
Cohen, M.X., 2014. Analyzing Neural Time Series Data: Theory and Practice. MIT.

Cooke, S.F., Bear, M.F., 2012. Stimulus-selective response plasticity in the visual cortex: an assay for the assessment of pathophysiology and treatment of cognitive impairment associated with psychiatric disorders. Biol. Psychiatry 71 (6), 487–495. http://doi.org/10.1016/j.biopsych.2011.09.006.

Çavuş, I., Reinhart, R.M.G., Roach, B.J., Gueorguieva, R., Teyler, T.J., Clapp, W.C., et al., 2012. Impaired visual cortical plasticity in schizophrenia. Biol. Psychiatry 71 (6), 512–520. http://doi.org/10.1016/j.biopsych.2012.01.013.

Delacre, M., & Klein, O. (2019). Routliers: Robust Outliers Detection. R package version 0.0.0.3.

Delorme, A., Makeig, S., 2004. EEGLAB: an open source toolbox for analysis of single-trial EEG dynamics including independent component analysis. J. Neurosci. Methods 134 (1), 9–21. http://doi.org/10.1016/j.jneumeth.2003.10.009.

Di Russo, F., Martínez, A., Sereno, M.I., Pitzalis, S., Hillyard, S.A., 2002. Cortical sources of the early components of the visual evoked potential. Hum. Brain Mapp. 15 (2), 95–111. http://doi.org/10.1002/hbm.10010.

D'Souza, D.C., Carson, R.E., Driesen, N., Johannesen, J., Ranganathan, M., Krystal, J.H.Yale GlyT1 Study Group, 2018. Dose-related target occupancy and effects on circuitry, behavior, and neuroplasticity of the glycine transporter-1 inhibitor PF-03463275 in healthy and schizophrenia subjects. Biological Psychiatry 84 (6), 413–421.

Elvsåshagen, T., Moberget, T., Bøen, E., Boye, B., Englin, N.O.A., Pedersen, P.Ø., et al., 2012. Evidence for impaired neocortical synaptic plasticity in bipolar II disorder. Biol. Psychiatry 71 (1), 68–74. http://doi.org/10.1016/j.biopsych.2011.09.026.

Forsyth, J.K., Bachman, P., Mathalon, D.H., Roach, B.J., Asarnow, R.F., 2015. Augmenting NMDA receptor signaling boosts experience-dependent neuroplasticity in the adult human brain. Proc. Natl. Acad. Sci. 112 (50), 15331–15336. http://doi.org/10.1073/pnas.1509262112.

Forsyth, J.K., Bachman, P., Mathalon, D.H., Roach, B.J., Ye, E., Asarnow, R.F., 2017. Effects of augmenting n-methyl-D-aspartate receptor signaling on working memory and experience-dependent plasticity in schizophrenia: an exploratory study using acute d-cycloserine. Schizophr. Bull. 43 (5), 1123–1133.

Fox, J., Weisberg, S., 2019. An {R} Companion to Applied Regression, 3rd Ed. Sage, Thousand Oaks CA.

Frenkel, M.Y., Sawtell, N.B., Diogo, A.C.M., Yoon, B., Neve, R.L., & Bear, M.F. (2006). Instructive effect of visual experience in mouse visual cortex, 51(3), 339–349. http://doi.org/10.1016/j.neuron.2006.06.026

Garren, S.T. (2019). jmuOutlier: permutation tests for nonparametric statistics. R package version 2.2.

de Gobbi-Porto, F.H., Fox, A.M., Tusch, E.S., Sorond, F., Mohammed, A.H., Daffner, K.R., 2015. In vivo evidence for neuroplasticity in older adults. Brain Res. Bull. 114, 56–61. http://doi.org/10.1016/j.brainresbull.2015.03.004.

Graham, F.K., Murray, G.M., 1977. Discordant effects of weak prestimulation on magnitude and latency of the reflex blink. Physiol. Psychol. 5 (1), 108–114.

Groppe, D.M., Urbach, T.P., Kutas, M., 2011. Mass univariate analysis of event-related brain potentials/fields I: a critical tutorial review. Psychophysiology 48 (12), 1711–1725. http://doi.org/10.1111/j.1469-8986.2011.01273.x.

Ioannidis, J.P.A., 2008. Why most discovered true associations are inflated. Epidemiology 19 (5), 640–648. http://doi.org/10.1097/EDE.0b013e31818131e7.

Jahshan, C., Wynn, J.K., Mathalon, D.H., Green, M.F., 2017. Cognitive correlates of visual neural plasticity in schizophrenia. Schizophr. Res. 190, 39–45. http://doi.org/10.1016/j.schres.2017.03.016.

Klöppel, S., Lauer, E., Peter, J., Minkova, L., Nissen, C., Normann, C., et al., 2015. LTP-like plasticity in the visual system and in the motor system appear related in young and healthy subjects. Front. Hum. Neurosci. 9 (695), 506. http://doi.org/10.3389/fnhum.2015.00506.

Li, J., Ji, L., 2005. Adjusting multiple testing in multilocus analyses using the eigenvalues of a correlation matrix. Heredity (Edinb) 95 (3), 221–227. http://doi.org/10.1038/sj.hdy.6800717.

Lisman, J., 2017. Glutamatergic synapses are structurally and biochemically complex because of multiple plasticity processes: long-term potentiation, long-term depression, short-term potentiation and scaling. Philos. Trans. R. Soc. Lond., B 372 (1715), 20160260. http://doi.org/10.1098/rstb.2016.0260.

Luders, E., Narr, K.L., Thompson, P.M., Rex, D.E., Jancke, L., Steinmetz, H., Toga, A.W., 2004. Gender differences in cortical complexity. Nature Neuroscience 7 (8), 799–800. doi:10.1038/nn1277.

McNair, N.A., Clapp, W.C., Hamm, J.P., Teyler, T.J., Corballis, M.C., Kirk, I.J., 2006. Spatial frequency-specific potentiation of human visual-evoked potentials. Neuroreport 17 (7), 739–741. http://doi.org/10.1097/01.wnr.0000215775.53732.9f.

Näätänen, R., Gaillard, A.W.K., Mäntysalo, S., 1978. Early selective-attention effect on evoked potential reinterpreted. Acta Psychol. (Amst) 42 (4), 313–329.

Normann, C., Schmitz, D., Fürmaier, A., Döing, C., Bach, M., 2007. Long-term plasticity of visually evoked potentials in humans is altered in major depression. Biol. Psychiatry 62 (5), 373–380. http://doi.org/10.1016/j.biopsych.2006.10.006.

R Core Team. (2019). R: a language and environment for statistical computing.

Regehr, W.G., 2012. Short-term presynaptic plasticity. Cold Spring Harb. Perspect. Biol. 4 (7), a005702. –a005702 http://doi.org/10.1101/cshperspect.a005702 .

Ross, R.M., McNair, N.A., Fairhall, S.L., Clapp, W.C., Hamm, J.P., Teyler, T.J., Kirk, I.J., 2008. Induction of orientation-specific LTP-like changes in human visual evoked potentials by rapid sensory stimulation. Brain Res. Bull. 76 (1–2), 97–101. http://doi.org/10.1016/j.brainresbull.2008.01.021.

Smallwood, N., Spriggs, M.J., Thompson, C.S., Wu, C.C., Hamm, J.P., Moreau, D., Kirk, I.J., 2015. Influence of physical activity on human sensory long-term potentiation. Journal of the International Neuropsychological Society 21, 831–840. http://doi.org/10.1017/S1355617715001095.

Schizophrenia Working Group of the Psychiatric Genomics Consortium, 2014. Biological insights from 108 schizophrenia-associated genetic loci. Nature 511 (7510), 421–427. http://doi.org/10.1038/nature13595.

Spriggs, M.J., Cadwallader, C.J., Hamm, J.P., Tippett, L.J., Kirk, I.J., 2017. Age-related alterations in human neocortical plasticity. Brain Res. Bull. 130, 53–59. http://doi.org/10.1016/j.brainresbull.2016.12.015.

Spriggs, M.J., Sumner, R.L., McMillan, R.L., Moran, R.J., Kirk, I.J., Muthukumaraswamy, S.D., 2018. Indexing sensory plasticity: evidence for distinct predictive coding and Hebbian learning mechanisms in the cerebral cortex. Neuroimage 176, 290–300. http://doi.org/10.1016/j.neuroimage.2018.04.060.

Spriggs, M.J., Thompson, C.S., Moreau, D., McNair, N.A., Wu, C.C., Lamb, Y.N., et al., 2019. Human sensory LTP predicts memory performance and is modulated by the BDNF Val66Met polymorphism. Front Hum Neurosci 13, 387. http://doi.org/10.3389/fnhum.2019.00022.

Stephan, K.E., Baldeweg, T., Friston, K.J., 2006. Synaptic plasticity and dysconnection in schizophrenia. Biol. Psychiatry 59 (10), 929–939. http://doi.org/10.1016/j.biopsych.2005.10.005.

Sumner, R.L., McMillan, R., Spriggs, M.J., Campbell, D., Malpas, G., Maxwell, E., Muthukumaraswamy, S.D., 2020. Ketamine enhances visual sensory evoked potential long-term potentiation in patients with major depressive disorder. Biol Psychiatry Cogn Neurosci Neuroimaging 5 (1), 45–55.

Sumner, R.L., Spriggs, M.J., McMillan, R.L., Sundram, F., Kirk, I.J., Muthukumaraswamy, S.D., 2018. Neural plasticity is modified over the human menstrual cycle: combined insight from sensory evoked potential LTP and repetition suppression. Neurobiol. Learn. Mem. 155, 422–434.

Takeuchi, T., Duszkiewicz, A.J., Morris, R.G.M., 2013. The synaptic plasticity and memory hypothesis: encoding, storage and persistence. Philos. Trans. R. Soc. Lond., B, Biol. Sci. 369 (1633), 20130288 –20130288.

Teyler, T.J., Hamm, J.P., Clapp, W.C., Johnson, B.W., Corballis, M.C., Kirk, I.J., 2005. Long-term potentiation of human visual evoked responses. Eur. J. Neurosci. 21 (7), 2045–2050. http://doi.org/10.1111/j.1460-9568.2005.04007.x.

Wilson, J.F., Lodhia, L., Courtney, D.P., Kirk, I.J., Hamm, J.P., 2017. Evidence of hyper-plasticity in adults with autism spectrum disorder. Research in Autism Spectrum Disorders 43-44, 40–52.

Wynn, J.K., Roach, B.J., McCleery, A., Marder, S.R., Mathalon, D.H., Green, M.F., 2019. Evaluating visual neuroplasticity with EEG in schizophrenia outpatients. Schizophr. Res. 212, 40–46. http://doi.org/10.1016/j.schres.2019.08.015.

Zak, N., Moberget, T., Bøen, E., Boye, B., Waage, T.R., Dietrichs, E., et al., 2018. Longitudinal and cross-sectional investigations of long-term potentiation-like cortical plasticity in bipolar disorder type II and healthy individuals. Transl Psychiatry 8 (1), 103. http://doi.org/10.1038/s41398-018-0151-5.